Armeniaspirol A: a novel anti-*Helicobacter pylori* agent

Jia Jia,[1,2] Chongwen Zhang,[1] Yaqi Liu,[3]
Yanqiang Huang,[1] Yuefan Bai,[1] Xudong Hang,[1]
Liping Zeng,[1] Dongqing Zhu[3] and Hongkai Bi[1,2] (iD)

[1]*Department of Pathogen Biology & Jiangsu Key Laboratory of Pathogen Biology & Helicobacter pylori Research Centre, Nanjing Medical University, Nanjing, Jiangsu, 211166, China.*
[2]*Department of Gastroenterology, Sir Run Run Hospital, Nanjing Medical University, Nanjing, Jiangsu, 211166, China.*
[3]*Key Laboratory of Combinatorial Biosynthesis and Drug Discovery Ministry of Education, School of Pharmaceutical Sciences, Wuhan University, Wuhan, Hubei, 430071, China.*

Summary

Antibiotic resistance in *Helicobacter pylori* has been growing worldwide with current treatment regimens. Development of new compounds for treatment of *H. pylori* infections is urgently required to achieve a successful eradication therapy in the future. Armeniaspirols, a novel class of natural products isolated from *Streptomyces armeniacus*, have been previously identified as antibacterial agents against Gram-positive pathogens. In this study, we found that armeniaspirol A (ARM1) exhibited potent antibacterial activity against *H. pylori*, including multidrug-resistant strains, with MIC range values of 4–16 μg ml^{-1}. The underlying mechanism of action of ARM1 against *H. pylori* involved the disruption of bacterial cell membranes. Also, ARM1 inhibited biofilm formation, eliminated preformed biofilms and killed biofilm-encased *H. pylori* in a dose-dependent manner. In a mouse model of multidrug-resistant *H. pylori* infection, dual therapy with ARM1 and omeprazole showed efficient *in vivo* killing efficacy comparable to the standard triple therapy, and induced negligible toxicity against normal tissues. Moreover, at acidic pH 2.5, ARM1 exhibited a much more potent anti-*H. pylori* activity than metronidazole. Thus, these findings demonstrated that ARM1

is a novel potent anti-*H. pylori* agent, which can be developed as a promising drug lead for treatment of *H. pylori* infections.

Introduction

Helicobacter pylori is a ubiquitous Gram-negative, spiral and microaerophilic bacterium that selectively colonizes in human gastric mucosa, and affects more than 50% of the world's population (Warren and Marshall, 1983; Peek and Blaser, 2002). It is closely associated with the incidence of chronic gastritis, peptic ulcers, gastric carcinoma and mucosa-associated lymphoid tissue (MALT) lymphomas (Amieva and Peek, 2016; Zhang *et al.*, 2016). In most cases, *H. pylori* infection is acquired in early childhood and adolescence, and persists lifelong if left untreated (Mamishi *et al.*, 2016). The eradication therapy of *H. pylori* infection has been recommended in all *H pylori*-positive patients with peptic ulcer disease by all of the consensus conferences around the world. It has also been proposed to reduce the risk of gastric cancer (Sugano *et al.*, 2015; Choi *et al.*, 2020). First-line treatment of *H. pylori* infection consists of triple and quadruple therapies. The standard triple treatment consists of a proton pump inhibitor (PPI) and two broad-spectrum antimicrobials (amoxicillin, clarithromycin, levofloxacin and metronidazole), while quadruple therapy contains one additional drug bismuth (Chey *et al.*, 2017; Georgopoulos and Papastergiou, 2020). However, worldwide increasing resistance to key antibiotics is currently the primary concern in the field of *H. pylori* infection, leading to a high incidence of failures in *H. pylori* eradication (Fabrega *et al.*, 2009; Papastergiou *et al.*, 2014). Results of a meta-analysis study in 2018 showed that the primary and secondary resistance rates to clarithromycin, metronidazole and levofloxacin have now reached alarming levels (≥ 15%) in almost all World Health Organization (WHO) regions (Savoldi *et al.*, 2018). Due to the rapid development of antibiotic resistance, the failure rate of triple therapy has increased to more than 20% in many parts of the world (Thung *et al.*, 2016). Therefore, there is a strong need to develop novel antibacterial strategies against *H. pylori*.

The development of drugs derived from natural microbial sources is receiving considerable attention particularly because of their potential to inhibit bacterial growth (Moloney, 2016). Halogenated pyrroles isolated from *Streptomyces* sp. have been shown to possess potent antimicrobial activities against a series of Gram-positive

Table 1. MICs of ARM1 and its derivatives against *H. pylori* standard strain G27 and multidrug-resistant strain Hp159.

Parent structure	Compound	R_1	R_2	R_3	R_4	MIC (μg ml^{-1}) G27	Hp159
	ARM1	H	CH$_3$	CH$_3$	Cl	8	8
	2	CH$_3$	H	CH$_3$	Cl	8	4
	3	CH$_3$	CH$_3$	CH$_3$	Cl	8	4
	7	H	CH$_3$	H	Cl	32	16
	8	CH$_3$	H	H	Cl	32	16
	9	CH$_3$	CH$_3$	H	Cl	16	16
	10	H	CH$_3$	H	H	8	8
	11	CH$_3$	H	H	H	16	8
	12	CH$_3$	CH$_3$	H	H	16	16
	13	H	CH$_3$	CH$_3$	H	4	8
	14	CH$_3$	H	CH$_3$	H	4	8
	15	CH$_3$	CH$_3$	CH$_3$	H	4	4
	4	H	CH$_3$	–	–	8	4
	5	CH$_3$	H	–	–	8	8
	6	CH$_3$	CH$_3$	–	–	8	16
	MTZ					2 (S)	16 (R)
	CLR					0.004 (S)	2 (R)
	LVX					0.5 (S)	8 (R)
	AMX					0.125 (S)	0.125 (S)

Breakpoints are according to EUCAST (European Committee on Antimicrobial Susceptibility Testing) guidelines. S, drug sensitive; R, drug resistant; MTZ, metronidazole; CLR, clarithromycin; LVX, levofloxacin; AMX, amoxicillin.

bacteria and fungi (Trew *et al.*, 2000; Hughes *et al.*, 2008). Armeniaspirols, with a unique chlorinated spiro [4.4]non-8-ene scaffold (Table 1), are a new class of natural antibacterial products isolated from *Streptomyces armeniacus* (Couturier *et al.*, 2012). In our recent work, we identified four enzymes involved in the biosynthesis of armeniaspirol A-C (1 – 3) isolated from *S. armeniacus* DSM 43125 and manipulated their activity to generate nine new analogues, 7–15 (Table 1) (Qiao *et al.*, 2019). Particularly, armeniaspirols 1–6 displayed potent activity against a range of multidrug-resistant Gram-positive bacterial pathogens, including *Staphylococcus aureus*, *Enterococcus faecium* and *Bacillus subtilis* (Couturier *et al.*, 2012; Dufour *et al.*, 2012; Qiao *et al.*, 2019). However, no inhibitory activity against Gram-negative bacteria, including *Acinetobacter baumannii*, *Pseudomonas aeruginosa*, *Klebsiella pneumonia*, *Salmonella typhimurium*, *Shigella dysenteriae* and *Escherichia coli*, was observed for all armeniaspirols 1–15 (Qiao *et al.*, 2019).

Based on this, the aim of the present study was to investigate whether armeniaspirols have anti-*H. pylori* activities. Herein we report that armeniaspirol A (ARM1) possesses a potent *in vitro* antibacterial activity against various standard and drug-resistant strains of *H. pylori*. ARM1 also showed better antibiofilm activity with killing biofilm-encased *H. pylori* cells than metronidazole. Furthermore, *in vivo* efficacy studies showed that oral administration of ARM1 plus omeprazole could significantly reduce *H. pylori* burden, with comparable efficacy to the triple-therapy approach. These findings indicate that ARM1 can be used as a potential antimicrobial agent for *H. pylori* clearance and treatment.

Results

ARM1 possesses potent antibacterial effect on drug-sensitive and -resistant H. pylori strains in vitro

The MICs of fifteen armeniaspirol derivatives against *H. pylori* standard strain G27 and multidrug-resistant strain Hp159 were 4–32 μg ml^{-1} (Table 1), suggesting that these compounds have potential anti-*H. pylori* abilities *in vitro*. Considering the highly available fermentation yield of ARM1 (approximately 1 mg l^{-1}) compared with other compounds (approximately 0.2–0.5 mg l^{-1}), we focus on it for further assessing the antibacterial activity against *H. pylori* clinical isolates. ARM1 showed similar antibacterial activity for all 13 clinical strains including antibiotic-susceptible and resistant isolates, with MIC values of 4–16 μg ml^{-1} (Table 2).

Time-dependent killing experiments were then performed with *H. pylori* G27 exposed to ARM1 to determine its effectiveness as a bactericidal agent. For quality control and comparative analyses, the antibiotic MTZ was also tested. Both compounds exhibited concentration-dependent and time-dependent killing kinetics (Fig. 1). With ARM1 at 1 × MIC, a 1-log decrease in cell count was observed at 8 h, followed by some increase in growth till 48 h, indicating no effect at this dose. At
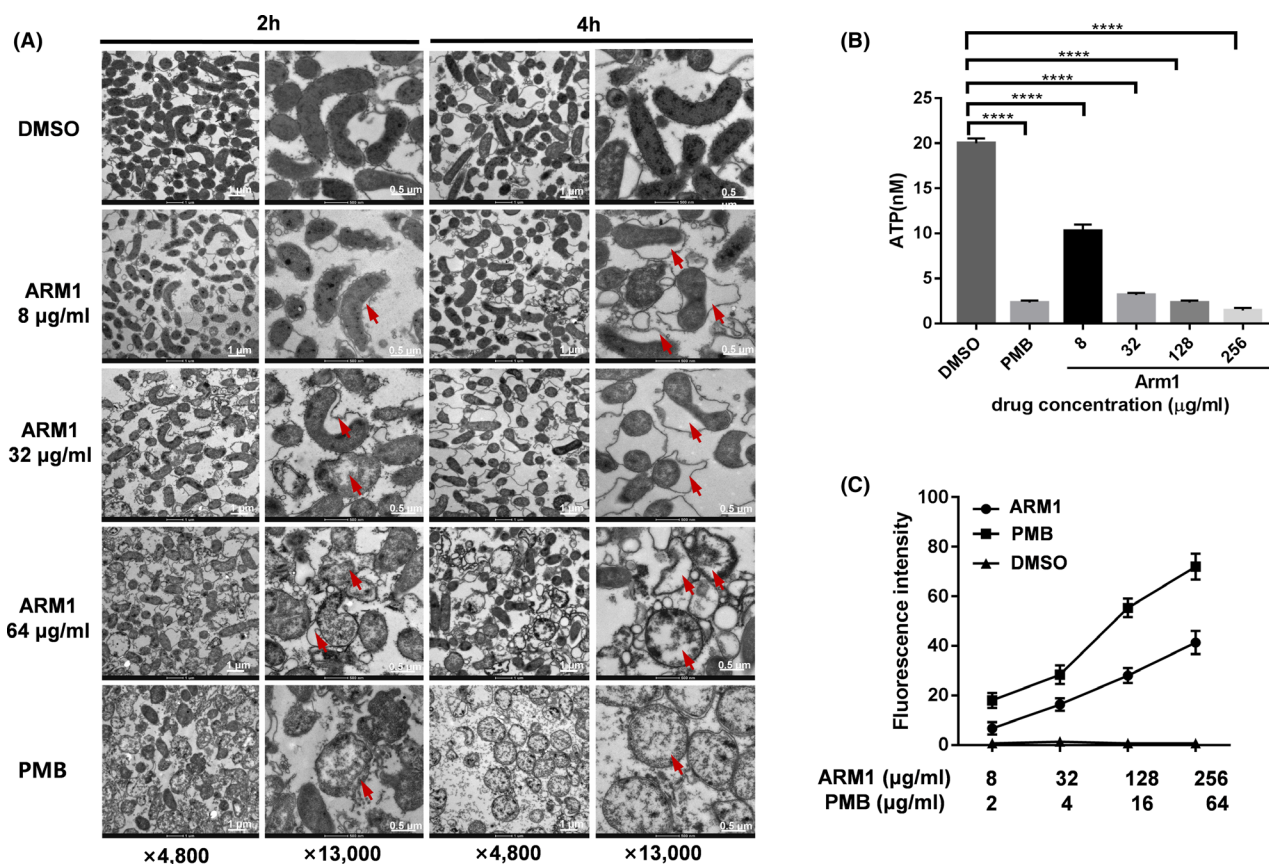
Fig. 2. ARM1 permeabilizes *H. pylori* cell membranes.

A. Morphology changes of *H. pylori* cells following exposure to DMSO, ARM1 or polymyxin B (PMB) observed by TEM. Membrane permeabilized agent PMB (10 μg ml^{-1}) served as a positive control which showed characteristically cell deformation and lysis with cytoplasmic contents leakage. Arrows indicate cell lysis, bleb formation, cell wall damage or separation between the cell wall and inner membrane. The data are representative images from two independent experiments.

B. Determination of intracellular ATP levels of *H. pylori* cells after exposure to various concentrations of ARM1. Statistical differences between the control (DMSO) and AMR1 treatment groups were analysed by one-way ANOVA followed by Dunnett's *t*-test (****$P < 0.0001$).

C. Uptake of *N*-phenylnapthylamine (NPN) by *H. pylori* G27 cells after 30 min treatment of DMSO (negative control), PMB (positive control) and various concentrations of ARM1. Data represent medians ± SD of the results from three independent experiments.

or intracellular ATP synthesis. We also used the hydrophobic fluorescence probe *N*-phenyl-1-naphthy-lamine (NPN) to examine the effect of ARM1 on the outer membrane of *H. pylori* in response to ARM1 treatment. *H. pylori* G27 treated with increasing concentrations of ARM1 showed a significant increase in the fluorescence signal of NPN, similar to that treated with polymyxin B, which disrupts the outer membrane permeability barrier (Fig. 2C), indicating that ARM1 permeabilized the outer membranes of *H. pylori*. Collectively, these data suggested that the mechanism of ARM1 action against *H. pylori* involved the disruption of bacterial cell membranes.

ARM1 has antibiofilm activity and kills biofilm-encased H. pylori

Biofilm formation has been suggested to play an important role in *H. pylori* colonization and resistance to

antibacterial therapy (Carron *et al.*, 2006; Yonezawa *et al.*, 2015; Hathroubi *et al.*, 2018). Thus, eradicating biofilms of *H. pylori* could become an effective strategy to improve the eradication rate. We first used the crystal violet assay to evaluate the ability of ARM1 to prevent biofilm formation. ARM1 and MTZ had similar biofilm inhibition pattern against *H. pylori*. Both even inhibited biofilm formation of *H. pylori* G27 at low concentrations (0.5 × MIC), and the biofilm formation could be reduced up to 54% and 49% at 1 × MIC respectively (Fig. 3A). Furthermore, preformed biofilms of *H. pylori* G27 were also eliminated by ARM1 in a dose-dependent manner. ARM1 at 4 × MIC disrupted the preformed biofilm of *H. pylori* by 66% (Fig. 3B).

The Alamar Blue assays were then performed to examine the effect of ARM1 on the cell viability of pre-formed biofilms. Compared with MTZ, ARM1 at 16 mg l^{-1} (2 × MIC) killed almost all *H. pylori* G27 cells within the
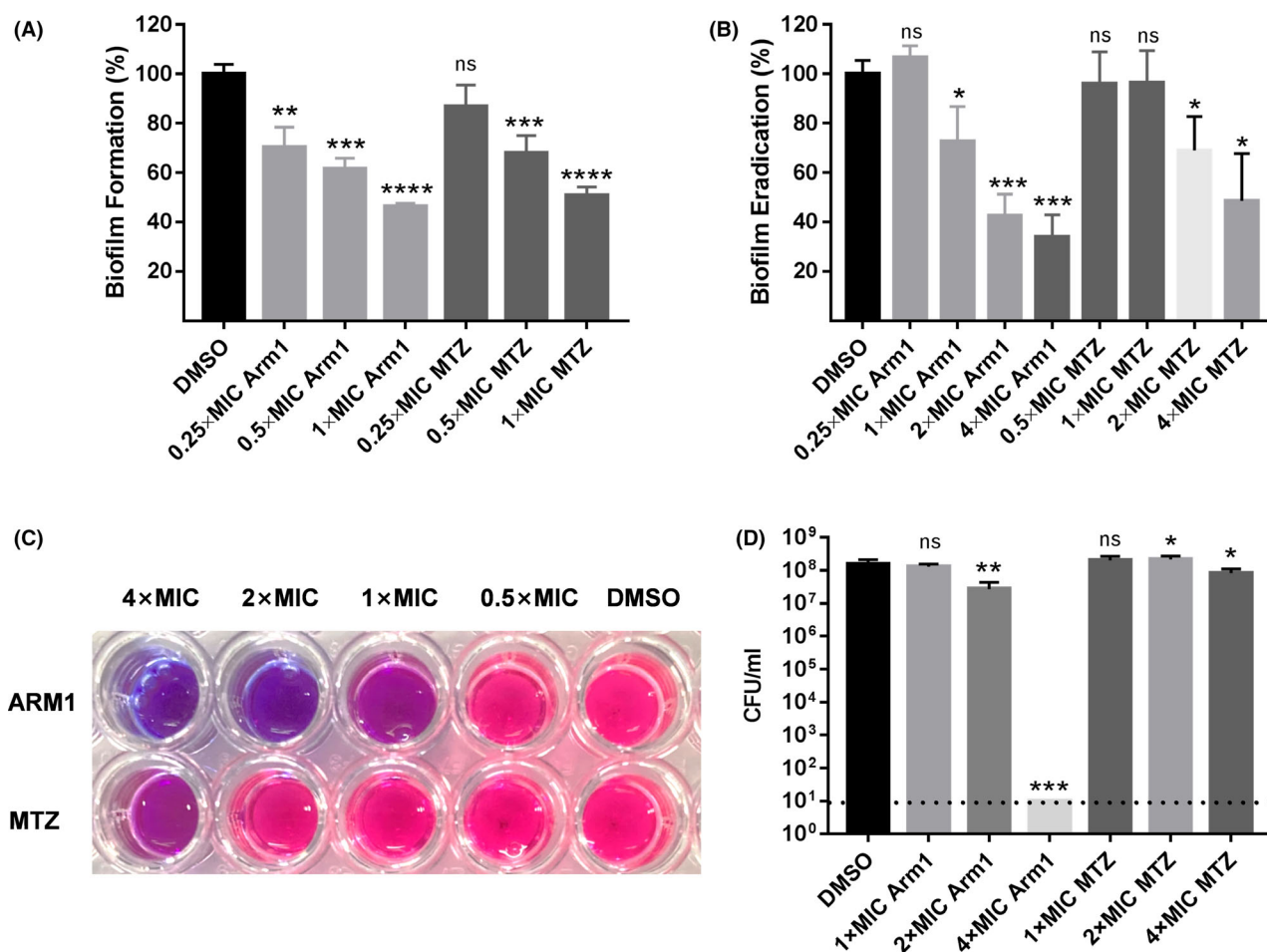
Fig. 3. Antibiofilm activity of ARM1. The ability of ARM1 to inhibit biofilm formation (A), and to eliminate preformed biofilms (B) of *H. pylori* G27 was tested using crystal violet assays. The impact on the cell viability of *H. pylori* G27 within biofilms by ARM1 was assessed by Alamar Blue assay (C) and viable colony count methods (D). MTZ and DMSO served as positive and negative controls respectively. Data are represented as averages $\pm$ SD of three independent experiments analysed by Student's *t*-test. If no colonies were present, calculations were made using the limit of detection. *$P < 0.05$; **$P < 0.01$; ***$P < 0.001$. 'ns' represents no significant difference ($P > 0.05$).

biofilms (Fig. 3C). The complete eradication was further confirmed by performing viable cell counts. As shown in Fig. 3D, treatment with ARM1 at 4 × MIC caused a > 7-log reduction in bacterial counts, which was much more effective than MTZ. Taken together, these data suggested that ARM1 was able to inhibit biofilm formation and to kill biofilm-encased *H. pylori*.

ARM1 kills H. pylori *in vivo*

The *in vivo* antibacterial activity of the ARM1 was evaluated in the mouse infection model (Fig. 4A). The mouse was infected by *H. pylori* BHKS159 (Huang *et al.*, 2019), a mouse-adapted multidrug-resistant strain, by oral gavage every other day for four times. At 3 weeks after inoculation, the mice were randomly divided into three groups and treated with phosphate-buffered saline (PBS) (control), triple therapy (omeprazole plus amoxicillin and

clarithromycin [OPZ + AC]) and dual therapy (omeprazole plus ARM1 [OPZ + ARM1]). In this study, therapeutic efficacy was evaluated by enumerating and comparing *H. pylori* counts in mouse stomach. Remarkably, after 5 day drug treatment, administration of OPZ + ARM1 (28.5 mg kg^{-1}) significantly impacted stomach bacteria load (Fig. 4B); the corresponding median colony-forming units (cfu) dropped significantly from 2.5×10^5 to 1.1×10^3 CFU g^{-1}, representing 99.56% inhibition of stomach colonization compared with the PBS group. Likewise, triple-therapy treatment also decreased the bacteria load to 1.3×10^3 CFU g^{-1}, showing similar bacteria-killing ability with the dual therapy with OPZ + ARM1 (Fig. 4B). Additionally, histopathological examination of fixed stomach sections revealed that OPZ + ARM1 treatment alleviated stomach inflammation with reduced infiltration of inflammatory cells into the stomach epithelial cells (Fig. 4C).
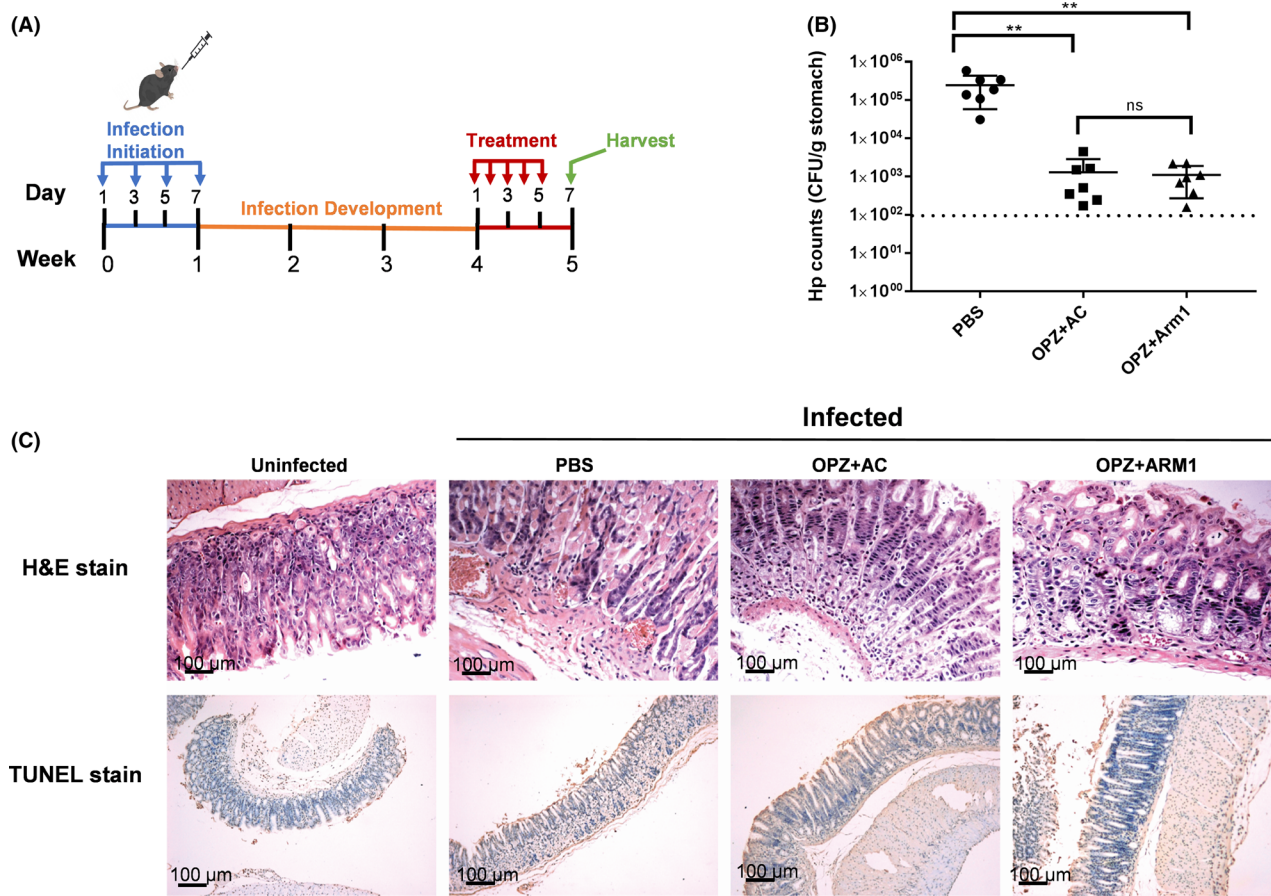
Fig. 4. *In vivo* effect of ARM1 on *H. pylori* infection in C57BL/6J mice.
A. The mice infection and treatment schedule utilized to investigate in vivo efficacy of ARM1 against *H. pylori* BHKS159.
B. Quantification of bacterial burden in the stomach of *H. pylori*-infected mice, euthanatized 48 h after the last treatment with PBS, triple therapy (OPZ + AC), omeprazole and ARM1 (OPZ + ARM1) respectively. Error bars represent the SD derived from 7 infected mice per group. If no colonies were present, calculations were made using the limit of detection (10^2 CFU g^{-1}). **$P < 0.01$. 'ns' represents no significant difference ($P > 0.05$).
C. Histological staining analysis of mice after the indicated treatments. Representative images of H&E or TUNEL stained stomach from infected mice receiving different treatments *in vivo*. TUNEL stain showed that OPZ + ARM1 treatment had the same safety level as control ($n \geq 5$, scale bar = 100 μm).

Moreover, OPZ + ARM1 administration did not show apparent gastric epithelial apoptosis compared to the PBS and OAC-treated groups analysed by the TUNEL assay (Fig. 4C), indicating that ARM1 did not induce obvious apoptosis *in vivo*. Taken collectively, these results suggested a high efficacy of ARM1 in clearance of drug-resistant *H. pylori in vivo*.

ARM1 performed potent antibacterial effect at acidic condition (pH = 2.5)

H. pylori colonizes the acidic gastric environment and survives brief exposure to pHs of < 4. We then re-evaluated the anti-*H. pylori* activity of ARM1 in an acid survival analysis to closely mimic gastric conditions. The experiment was carried out at pH 2.5 in the presence of 10 mM Urea. When the bacteria were treated with

ARM1 and MTZ at a lower concentration (0.5 μg ml^{-1}), both had no significant effect on the survival rates compared with the DMSO group (Fig. 5). However, notable bacterial killing was achieved by ARM1 at 2 and 8 μg ml^{-1}. Especially, when treated with 8 μg ml^{-1}, the survival rate of the ARM1-treated group was 0.0013%, 3 orders of magnitude lower than that of MTZ-treated group (Fig. 5). Thus, ARM1 exhibited much more potent anti-*H. pylori* activity under extremely acidic conditions than MTZ.

Safety evaluation of ARM1

At last, the toxicity of ARM1 was investigated. ARM1 exhibited no significant cytotoxicity to human normal hepatocyte LO_2 cells (IC_{50} = 147.5 μg ml^{-1}) with 96.5% survival rate when treated with 100 μg ml^{-1} of ARM1

Fig. 5. The survival rate of *H. pylori* G27 after incubation with ARM1 or MTZ for 30 min at pH 2.5. ARM1 or MTZ at various concentrations was incubated with *H. pylori* 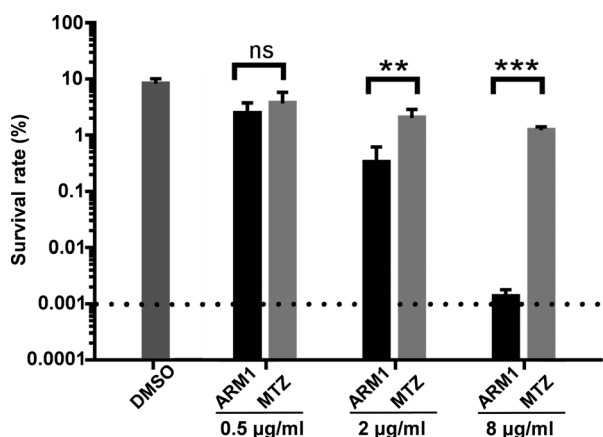G27 in BHI broth (pH2.5) in the presence of fresh urea (10 mM) and 10% FBS. The bacterial count was determined by counting colony-forming units (cfu) of live bacteria with agar plating. The data are represented as average ± SD of three independent experiments and analysed by Student's *t*-test. **$P < 0.01$, ***$P < 0.001$. 'ns' represents no significant difference ($P > 0.05$).

(Fig. S3). Moreover, the low toxicity of ARM1 was further validated by treatment with 10 times the effective dosage *in vivo*. Within 5 day overdose treatment of ARM1, no serious adverse effects such as diarrhoea and loss of appetite or body weight were observed (Fig. S4A). Also, there were no obvious differences in the histopathologic examination of mouse major organs including liver, kidney, spleen and stomach treated with ARM1 and PBS (Fig. S4B), which supported that ARM1 had low toxicity *in vivo*. In addition, the drug-like properties of ARM1 were predicted by SwissADME *in silico*. ARM1 showed excellent drug-like properties, including high oral absorption, high bioavailability and moderate toxicity (Table S1). Taken together, ARM1 could be developed as a potential anti-*H. pylori* therapeutic agent with minimal toxicity profiles.

Discussion

In recent years, there has become more challenging to the clinical treatment of *H. pylori* due to the prevalence of antibiotic resistance (Hu *et al.*, 2016; Zanotti and Cendron, 2019; Pichon *et al.*, 2020). Hence, the discovery and development of new anti-*H. pylori* agents without cross-resistance to current drugs are highly impending and important. In this study, we demonstrated that ARM1, a natural product isolated from *S. armeniacus*, targets *H. pylori in vivo* and *in vitro* as a bactericidal agent. A comparable killing efficacy of dual therapy (ARM1 plus PPI) was evaluated in reducing *H. pylori* bacterial loads in the stomach of drug-resistant *H. pylori*-

infected mice, compared with the current worldwide standard treatment, triple therapy. In addition, an additive effect between ARM1 and some conventional antibiotic against *H. pylori* was found (Table S2), indicated that ARM1 could be developed as a good drug synergist candidate in the triple-therapy regimen used in clinical practice for future.

H. pylori produces a well-structured biofilm, which can impact the efficacy of antibiotic treatment and clearance by the host immune systems (Cammarota *et al.*, 2012; Hathroubi *et al.*, 2018). Thus, targeting *H. pylori* biofilm infections can provide an effective strategy to overcome *H. pylori* eradication treatment failures. In the present study, ARM1 alone not only prevented *H. pylori* biofilm formation but also eliminated the embedded bacteria in the biofilm. Moreover, the killing efficacy of ARM1 was even superior to that of the clinical drug MTZ. Such compound with antibiofilm activity might provide advantages in resolving multidrug-resistant *H. pylori* infections.

As demonstrated in our study, ARM1 permeabilized and disrupted the outer and inner membranes of *H. pylori*, resulting in a rapid killing effect. The highly destructive action for bacterial killing may explain the low tendency to develop resistance against *H. pylori* (Xu *et al.*, 2017; Huang *et al.*, 2019). In addition, the biofilm formation of *H. pylori* has been suggested to be highly associated with outer membrane proteins (Yonezawa *et al.*, 2017). Therefore, the membrane structural disruption caused by ARM1 treatment could also probably destabilize membrane proteins and thus induce biofilm collapse.

Based on previous studies, armeniaspirols demonstrated no antimicrobial activity against many Gram-negative bacteria (Couturier *et al.*, 2012; Qiao *et al.*, 2019). Thus, besides the cell membrane disrupting mode, we speculate there may also have alternative mechanisms for the bactericidal activity of armeniaspirole against *H. pylori*. Therefore, ARM1 likely targets a specific *H. pylori* protein absent in other Gram-negative bacteria. It should be also mentioned that under acidic condition (pH = 2.5), ARM1 showed much more potent anti-*H. pylori* activity than MTZ in the presence of urea (Fig. 5). This stronger antibacterial activity of ARM1 should not be attributed to changes in chemical structure under acidic condition, since the compound remains stable when exposed to pH2.5 (data not shown). *H. pylori* can utilize a complex and robust acid resistance system centred around the nickel enzyme urease, to survive the harsh acidic conditions of the stomach (Scott *et al.*, 2002; Krulwich *et al.*, 2011). It is highly possible that ARM1 interfere with this survival strategy in the acidic conditions, thus reducing survival rate of *H. pylori*. In view of the fact that the complex acid resistance system involves a variety of proteins, even unknown, ARM1

might act by regulating the urease expression and urease maturation or inhibiting its activity via binding to distinct proteins. Taken together, the robust anti-*H. pylori* activity conferred by ARM1 can be explained by the unique capability of ARM1 to disrupt membrane integrity and to suppress the acid resistance of *H. pylori*.

In summary, we report that ARM1, a natural product isolated from *S. armeniacus*, showed potent antimicrobial activity against *H. pylori* both *in vivo* and *in vitro*. It is a possible drug candidate not only inhibiting planktonic growth and biofilm formation but also disrupting the mature biofilm by permeabilizing bacterial membranes. Moreover, the early toxicity and safety evaluations also show that ARM1 exhibits a relative safety index. ARM1 might provide a promising drug lead for the development of anti-*H. pylori* therapy.

Experimental procedures

Chemicals

The cultivation of *S. armeniacus* strains and the purification of the compounds from the culture were carried out as previously described (Qiao *et al.*, 2019). The *S. armeniacus* strains (the wild-type strain DSM 43125 and mutant strains) were cultured in the liquid ISP-2 medium (0.4% yeast extract, 1% malt extract, 0.4% glucose, pH 7.0) containing 2 g l^{-1} CaCO$_3$ at 30°C and 200 rpm for 3 days. Then, 10% (v/v) of the culture was transferred in 50 ml of fresh ISP-2 medium and fermented at 30°C and 200 rpm for 6 days. The culture was separated from the biomass fraction and the supernatant fraction by centrifugation. The supernatant fraction was extracted with an equal volume of ethyl acetate twice. The biomass fraction was extracted with methanol, disrupted by sonication and centrifuged to remove the cell debris. The retained supernatant was concentrated on a rotovap, resuspended in water and extracted with an equal volume of ethyl acetate twice. The combined organic extracts were dried over anhydrous Na$_2$SO$_4$, filtered and concentrated on a rotovap. The residue was resuspended in methanol and filtered with a microporous membrane (0.22 μm, nylon). The compounds were purified first by using HPLC (Beijing QingBoHua Technologies, Beijing, China) with a Daisogel C18 reversed-phase HPLC column (250 × 20 mm, 10 μm). The HPLC conditions (mobile phase A: water; mobile phase B: methanol; UV detection λ:300 nm) were as follows: 10−90% B for 35 min, 90% B for 15 min, 90−10% B for 5 min and 10% B for 10 min at a flow rate of 10 ml min^{-1}. The obtained compounds were concentrated on a rotovap and further purified by using HPLC (Shimadzu, SPD-M20A/LC-20AT, Kyoto, Japan) with a Thermo Scientific C18 reversed-phase HPLC column (250 × 10 mm, 8 μm). The HPLC conditions (mobile phase A: water; mobile phase B: acetonitrile; UV detection λ: 300 nm) were as follows: 70% B for 30 min. The purified compounds were concentrated on a rotovap and dried on a freeze-dryer. 70 mg ARM1 (C$_{18}$H$_{19}$Cl$_2$NO$_4$; UV/vis λ$_{max}$ 208, 232, 299; HR-ESI-MS *m/z* 382.06818 ([M − H] $^-$, calcd *m/z* 382.06129) was purified from the culture of the wild-type strain DSM 43125 approximately 71 L. The following strains were cultured about 2–4 l respectively to purify the compounds **2-15** (approximately 1 mg each compound) used in this study : the wild-type strain DSM 43125 for **2-3**, the Δ*arm9*Δ*arm15* mutant strain QY13 for **4-6**, the Δ*arm16* mutant strain QY6 for **7-9** and the Δ*arm9* mutant strain QY4 for **10-15**.

Bacterial strains and culture media

H. pylori strains G27 (Baldwin *et al.*, 2007), Hp159 (Huang *et al.*, 2019) and 13 clinical isolates were used in this study and were routinely cultured either in brain heart infusion (BHI) broth (Becton, Dickinson, Sparks, MD, USA) medium containing 10% fetal calf serum (FCS) or in Columbia blood agar (Oxoid, Basingstoke, UK) plates containing 5% FCS, supplemented with Dent selective supplement (Oxoid). All of the plates or media were incubated at 37°C for 48 to 72 h under microaerophilic conditions (10% CO$_2$, 85% N$_2$, and 5% O$_2$ and 90% relative humidity) using a double-gas CO$_2$ incubator (Binder, model CB160, Tuttlingen, Germany). A total of 13 clinical strains of *H. pylori* were isolated from biopsy samples from patients with gastric cancer or gastric ulcer, obtained from the First Affiliated Hospital of Nanchang University and the First Affiliated Hospital of Nanjing Medical University, China, using standard protocols. The strains were identified based on colony appearance, Gram staining and positive reactions in the rapid urease test.

Drug susceptibility test

Antibacterial activities were evaluated by minimum inhibitory concentration (MIC) determination. Briefly, twofold serial dilutions of compounds were prepared in a 96-well microtitre plate containing 100 μl of BHI broth containing 10% FCS. An overnight *H. pylori* liquid culture was diluted in BHI broth and was inoculated into each well with a final concentration of 5 × 10^5 CFU ml^{-1}. The plates were incubated for 2 days in a microaerophilic atmosphere at 37°C. After incubation, the plates were examined visually, and the MIC was determined to be the lowest concentration with no turbidity in well. For quality control and comparative analysis, the antibiotic metronidazole was also tested with each batch of ARM1. All MIC assays were performed in at least triplicate.

Checkerboard microdilution assay

The standard checkerboard microdilution assay was used for evaluation of antimicrobial interactions between ARM1 and each antibiotic (AMX, CTR, LVX or MTZ) against *H. pylori* strains (Tanaka *et al.*, 2002). The test compounds represented by each antibiotic were serially diluted on the x-axis, ranging from 1 to $1/64 \times$ MIC, with increasing concentrations of ARM1 ranging from 1/32 to $1 \times$ MIC on the y-axis. For evaluation of synergistic effect of ARM1 (A) with the antibiotic tested (B), the fractional inhibitory concentrations (FICs) were calculated as follows: $\sum FIC = FIC_A + FIC_B$ where $FIC_A = MIC_A$ (in the presence of B)/MIC_A (alone), and $FIC_B = MIC_B$ (in the presence of A)/MIC_B (alone). The FIC indices were interpreted as follows: ≤ 0.5, synergy; 0.5–1, additive; 1–4.0, indifference; >4.0, antagonism. All MIC determinations were performed in triplicate for each strain.

Time-kill kinetics assay

10 ml of BHI containing 10% FCS in the presence of ARM1 (at $1\times$, $2\times$, $4\times$, or $8 \times$ MIC) or an equivalent amount of DMSO (which served as a vehicle control) was inoculated with *H. pylori* strain G27 obtained from an overnight culture to yield an initial cell density of $\sim 10^6$ CFU ml^{-1}. The culture was shaken at 150 rpm at 37°C inside the double-gas CO_2 incubator as stated before. At different time points (0, 2, 4, 8, 12, 24 and 48 h), aliquots (100 μl) of culture were taken out to monitor the growth by direct microscopic examination, and the viable cells were counted by inoculating 10-fold serially diluted suspensions onto Columbia blood agar plates. Colonies were counted after 4 days of incubation, and the bactericidal activities were assessed in terms of decrease in cell count (CFU ml^{-1}). The rate and extent of killing were determined by plotting viable counts (log_{10} CFU ml^{-1}) against time (h).

Plasma membrane permeability assay

The intracellular ATP level was determined as an indicator of plasma membrane permeability. Briefly, an overnight liquid culture of *H. pylori* G27 was diluted to an OD600 of 0.3, and the bacterial cells were treated with polymyxin B (10 μg ml^{-1}) or ARM1 (8, 16, 128 and 256 μg ml^{-1}) for 30min. An equivalent amount of DMSO was used as a vehicle control. After treatment, each bacterial suspension was centrifuged, the supernatant was separated from the cell pellet, and the cell pellet was resuspended in 1 ml of PBS. 100 μl aliquot of Bac-Titer-Glo reagent in the microbial cell viability assay kit (Promega, Madison, WI, USA) with 500 μg of lysostaphin was added to the resuspended cell pellet. The

mixture was shaken for 2 min, and luminescence was determined by a Synergy HTX multimode microplate reader (BioTek Instruments, Winooski, VT, USA). The concentration of ATP was determined by comparison to the luminescence obtained from the addition of the Bac-Titer-Glo reagent to an ATP standard curve.

Outer membrane permeability assay

NPN uptake assays were performed to determine the ability of ARM1 to permeabilize *H. pylori* outer membranes. Briefly, an overnight liquid culture of *H. pylori* G27 was harvested by centrifugation (4700 rpm, 10 min), washed twice in 5 mM 4-(2-hydroxyethyl)-1-piperazineethanesulfonic acid (HEPES) buffer (pH7.4) and then resuspended to an OD at 600 nm of 1 in 5 mM HEPES. Aliquots (100 μl) of the cell suspension were added to each well of 96-well microtitre plates containing 50 μl of ARM1 at various concentrations (8, 32, 128 and 256 μg ml^{-1}), while the polymyxin B and DMSO served as positive and negative controls respectively. After addition of 50μl NPN (40 μM), measurements were implemented taken after 30 min incubation at 37°C. Fluorescence measurements were taken using a Synergy HTX multimode microplate reader with an excitation wavelength of 350 nm and an emission wavelength of 420 nm. All NPN assays were performed in triplicate.

The antibiofilm assay

Biofilm formation assays were carried out as described previously (Hathroubi, et al., 2018), with small modification. *H. pylori* G27 was grown overnight, diluted to an optical density at 600 nm (OD600) of 0.15 with fresh Brucella broth containing 10% FCS and then used to fill triplicate wells of a sterile 96-well polystyrene microtitre plate. Various doses of ARM1 or metronidazole (MTZ, served as a positive control) were added to the wells above and an equivalent amount of DMSO was used as a vehicle control. Following 48 h of static incubation under microaerobic and 37°C, the culture medium was removed by aspiration, and the wells were washed twice with phosphate-buffered saline (PBS). Plates were incubated for 10 min at 37°C for dry. The wells were then filled with 250 μl of crystal violet (0.1% wt/vol), and biofilm inhibition was measured using the crystal violet staining method (Hathroubi *et al.*, 2018). To assess the ability of ARM1 to eradicate preformed biofilms, *H. pylori* G27 cells were cultured in microtitre plates for 2 days to allow for biofilm formation, and the medium was aspirated and then washed with PBS twice. Fresh Brucella broth containing 10% FCS and various doses of ARM1 or MTZ were added to the wells for another 24 h. The dispersal of mature biofilms was measured using the crystal violet staining method.

Quantifying effect of ARM1 on bacterial viability in biofilms

The bacterial viability within the biofilm was determined by Alamar Blue assay (Pettit *et al.*, 2005), which is a colorimetric assay involving the cellular reduction of a blue phenoxazin dye, resazurin to the pink fluorescent compound resorufin. Biofilms of the *H. pylori* G27 cells were prepared and treated followed by 24 h under microaerobic conditions described in the previous section. First, 10% Alamar Blue solution was added to each well. Plates were then incubated for 2 h at room temperature in the dark, and images were taken by a camera. The resorufin fluorescence was measured ($\lambda_{excitation}$, 530 nm; $\lambda_{emission}$, 590 nm) thereafter using a Synergy HTX multimode microplate reader. The fluorescence values of the samples were corrected by subtracting the average fluorescence value of Alamar Blue in uninoculated wells (blank). The percentage of surviving biofilm cells was calculated relative to the control treatment.

The effect of ARM1 on the cell viability of preformed biofilms was also investigated using colony count methods. Biofilms of the *H. pylori* G27 cells were prepared and treated followed by 24 h under microaerobic conditions described in the previous section. After incubation, additives were removed, and the biofilms were detached by scraping wells completely with a 200 μl pipette tip across the well. The scraped biofilms were then homogenized in solution by repeatedly pipetting the solution several times. Finally, the homogenized biofilm suspensions were serially diluted, spread out onto Columbia blood agar plates containing Dent supplement, and then incubated at 37°C under microaerobic conditions for 4 days. Viable bacterial colonies on plates were enumerated and expressed as CFU ml^{-1}.

Drug resistance study

H. pylori G27 was inoculated with fresh BHI containing 10% FCS and incubated at 37°C under continuous shaking. Cells were grown to log phase and dispensed into 96-well microtitre plates with 100 μl fresh medium per well (adjusted to approximately 2×10^6 cells). Metronidazole or ARM1 was added at a concentration of $0.5 \times$ MIC. After a 3 day incubation at 37°C under continuous shaking, growth was determined with a microplate reader at an optical density at 600 nm, and cells were used to inoculate the subsequent cultures. Alterations of MICs were recorded after every cycle during the continued exposure of 27 days with nine cycles of repetition. All measurements were performed with biological replicates.

Antibactericidal activity of ARM1 under acidic condition (pH 2.5)

H. pylori G27 was grown overnight, and diluted to an optical density at 600 nm (OD600) of 0.3 with 1 ml fresh BHI broth containing 10% FCS and 10mM Urea (adjusted to pH 2.5 with HCl). Various doses of ARM1 or metronidazole (MTZ, served as a positive control) were added to the medium above, and an equivalent amount of DMSO was used as a vehicle control. After 30 min of incubation in a microaerobic environment, the samples were harvested by centrifugation, washed once with PBS and resuspended with fresh BHI. The homogenate was serially diluted and spotted onto a Columbia blood agar plate supplemented with Dent selective supplement. The plates were then incubated at 37°C under microaerobic conditions for 4–5 days, and bacterial colonies were enumerated, and acid survival was expressed as a percentage of the number of viable cells after incubation at pH 2.5 relative to that before the challenge.

Cytotoxicity in LO$_2$ cell line

The *in vitro* cytotoxicity investigation was carried out by CCK-8 assays according to the manufacturer's instructions. Confluent human normal liver cells LO$_2$ (American Type Culture Collection, ATCC) in good condition were cultured in 96-well plates (5×10^3 cells per well) with RPMI 1640 medium containing 10% FBS and treated with ARM1 at various concentrations (16, 32, 64, 128 and 256 μg ml^{-1}) for 48 h. Then, the absorbance of each well at 490 nm was measured by a Synergy HTX multimode microplate reader. The inhibition rate and cell viability were normalized by the value of the DMSO-treated cells. The IC 50 value was calculated using GraphPad Prism 6 software (San Diego, CA, USA).

Transmission electron microscopy

The effects of ARM1 on the cell structure of *H. pylori* G27 were examined with TEM. Sample processing was performed essentially according to a published procedure (Hathroubi *et al.*, 2020). Briefly, an overnight culture of *H. pylori* G27 was treated with ARM1 (8, 32 and 64 μg ml^{-1}) and polymyxin B (10 μg ml^{-1}) served as positive control incubated for 2 h. PBS was used as a negative control. Samples were centrifuged at 1000 g for 10 min and bacterial pellets fixed by resuspending in 2% glutaraldehyde in 0.1 M sodium cacodylate buffer (pH 7.4). Bacterial pellets were then embedded in 2% agarose and postfixed with 1% osmium tetroxide overnight at room temperature. After washing, samples were dehydrated multiple times in increasing concentrations of ethanol and embedded in Durcupan resin (Sigma-

Aldrich, St. Louis, MO, USA). Fifty-five-nanometer sections were examined by a JEM-1200 transmission electron microscope (JEOL; Akishima, Tokyo, Japan).

Anti-H. pylori *efficacy* in vivo

Six-week-old specific-pathogen-free female C57BL/6 mice were used for this study. Each mouse was administered intragastrically with 0.4 ml of ~ 1×10^9 CFU ml^{-1} *H. pylori* BHKS159 every 48 h, repeated four times (on days 1, 3, 5 and 7 respectively). At 3 weeks after inoculation, the mice were randomly assigned to three treatment groups ($n = 7$) to treat as follows: ARM1 plus omeprazole, triple therapy or PBS. Omeprazole (400 μmol kg^{-1} day^{-1}) was fed through oral gavage 30 min before the administration of the assigned treatments. ARM1 (28.5 mg kg^{-1}) and triple-therapy formulation (amoxicillin 28.5 mg kg^{-1} and clarithromycin 14.3 mg kg^{-1}) were administered once daily for a consecutive 5 days by oral gavage. The control group received an equivalent volume of PBS. Forty-eight hours after the last treatment, mice were euthanized. The stomach, the liver, the spleen and the kidney were harvested from the abdominal cavity. The stomach was cut along the greater curvature, and the gastric content was removed and rinsed with BHI. The stomachs were cut into two longitudinal sections, used for assessment of bacterial colonization and histology/epithelial apoptosis, as described previously (Huang *et al.*, 2019). Mouse body weight was monitored every day daily. For bacterial colonization, a gastric tissue section was suspended in 1 ml BHI and homogenized for *H. pylori* recovery. The homogenate was serially diluted and spotted onto a Columbia agar plate containing vancomycin (20 μg ml^{-1}), amphotericin (2 μg ml^{-1}) and bacitracin (30 μg ml^{-1}). The plates were then incubated at 37°C under microaerobic conditions for 4–5 days, and bacterial colonies were enumerated, and the outcome was expressed as cfu per gram of stomach.

In vivo *toxicity study*

Animal studies were approved by the Institutional Animal Care and Use Committee (IACUC) of Nanjing Medical University (NJMU) and conducted in accordance with the international standards for animal welfare and institutional guidelines. Mice were obtained from the Animal Core Facility at NJMU and housed at the same place. ARM1 safety was evaluated *in vivo* by treatment of ARM1 overdose (285 mg kg^{-1}, 10-fold effective dosage) in C57BL/6 female mice ($n = 6$) at 6–8 week of age. Mice were given a daily gavage of ARM1 or PBS for 5 consecutive days. Mice were sacrificed on day 7, and the stomach, the liver, the spleen and the kidney were harvested from the abdominal cavity for histological analysis. The longitudinal sections of each tissue were fixed in buffered paraffin, embedded in paraffin wax, sectioned at 5 μm and stained with haematoxylin and eosin (H&E) to analyse tissue inflammation. Mouse body weight was monitored during the experiment period by weighing the mice daily.

Statistical analysis

Statistical analyses were performed, and graphs were generated by using Graphpad prism 7.0 version (San Diego, CA, USA). For all experiments, statistical analyses were determined with Student's *t*-test. A *P* value of < 0.05 was considered significance statistical difference.

Conflict of interest

All authors have no conflict of interest to declare.

References

Amieva, M., and Peek, R.M. Jr (2016) Pathobiology of *Helicobacter pylori*-induced gastric cancer. *Gastroenterology* **150:** 64–78.

Baldwin, D.N., Shepherd, B., Kraemer, P., Hall, M.K., Sycuro, L.K., Pinto-Santini, D.M., and Salama, N.R. (2007) Identification of *Helicobacter pylori* genes that contribute to stomach colonization. *Infect Immun* **75:** 1005–1016.

Cammarota, G., Sanguinetti, M., Gallo, A., and Posteraro, B. (2012) Review article: biofilm formation by Helicobacter pylori as a target for eradication of resistant infection. *Aliment Pharmacol Ther* **36:** 222–230.

Carron, M.A., Tran, V.R., Sugawa, C., and Coticchia, J.M. (2006) Identification of *Helicobacter pylori* biofilms in human gastric mucosa. *J Gastrointest Surg* **10:** 712–717.

Chey, W.D., Leontiadis, G.I., Howden, C.W., and Moss, S.F. (2017) ACG clinical guideline: treatment of *Helicobacter pylori* infection. *Am J Gastroenterol* **112:** 212–239.

Choi, I.J., Kim, C.G., Lee, J.Y., Kim, Y.I., Kook, M.C., Park, B., and Joo, J. (2020) Family history of gastric cancer

and *Helicobacter pylori* treatment. *N Engl J Med* **382:** 427–436.

Couturier, C., Bauer, A., Rey, A., Schroif-Dufour, C., and Broenstrup, M. (2012) Armeniaspiroles, a new class of antibacterials: Antibacterial activities and total synthesis of 5-chloro-Armeniaspirole A. *Bioorg Med Chem Lett* **22:** 6292–6296.

Dufour, C., Wink, J., Kurz, M., Kogler, H., Olivan, H., Sable, S., *et al.* (2012) Isolation and structural elucidation of armeniaspirols A-C: potent antibiotics against gram-positive pathogens. *Chemistry* **18:** 16123–16128.

Fabrega, A., Madurga, S., Giralt, E., and Vila, J. (2009) Mechanism of action of and resistance to quinolones. *Microb Biotechnol* **2:** 40–61.

Georgopoulos, S., and Papastergiou, V. (2020) An update on current and advancing pharmacotherapy options for the treatment of *H. pylori* infection. *Expert Opin Pharmacother* **12:** 1–13.

Hathroubi, S., Servetas, S.L., Windham, I., Merrell, D.S., and Ottemann, K.M. (2018) *Helicobacter pylori* biofilm formation and its potential role in pathogenesis. *Microbiol Mol Biol Rev* **82:** e00001–18.

Hathroubi, S., Zerebinski, J., Clarke, A., and Ottemann, K.M. (2020) *Helicobacter pylori* biofilm confers antibiotic tolerance in part via a protein-dependent mechanism. *Antibiotics (Basel)* **9:** 355.

Hu, Y., Zhang, M., Lu, B., and Dai, J. (2016) *Helicobacter pylori* and antibiotic resistance. A continuing and intractable problem. *Helicobacter* **21:** 349–363.

Huang, Y., Hang, X., Jiang, X., Zeng, L., Jia, J., Xie, Y., *et al.* (2019) In vitro and in vivo activities of zinc linolenate, a selective antibacterial agent against *Helicobacter pylori*. *Antimicrob Agents Chemother* **63:** e00004–19.

Hughes, C.C., Prieto-Davo, A., Jensen, P.R., and Fenical, W. (2008) The marinopyrroles, antibiotics of an unprecedented structure class from a marine *Streptomyces* sp. *Org Lett* **10:** 629–631.

Krulwich, T.A., Sachs, G., and Padan, E. (2011) Molecular aspects of bacterial pH sensing and homeostasis. *Nat Rev Microbiol* **9:** 330–343.

Mamishi, S., Eshaghi, H., Mahmoudi, S., Bahador, A., Hosseinpour Sadeghi, R., Najafi, M., *et al.* (2016) Intrafamilial transmission of *Helicobacter pylori*: genotyping of faecal samples. *Br J Biomed Sci* **73:** 38–43.

Moloney, M.G. (2016) Natural products as a source for novel antibiotics. *Trends Pharmacol Sci* **37:** 689–701.

Papastergiou, V., Georgopoulos, S.D., and Karatapanis, S. (2014) Treatment of *Helicobacter pylori* infection: meeting the challenge of antimicrobial resistance. *World J Gastroenterol* **20:** 9898–9911.

Peek, R.M. Jr, and Blaser, M.J. (2002) *Helicobacter pylori* and gastrointestinal tract adenocarcinomas. *Nat Rev Cancer* **2:** 28–37.

Pettit, R.K., Weber, C.A., Kean, M.J., Hoffmann, H., Pettit, G.R., Tan, R., *et al.* (2005) Microplate Alamar blue assay for *Staphylococcus epidermidis* biofilm susceptibility testing. *Antimicrob Agents Chemother* **49:** 2612–2617.

Pichon, M., Broutin, L., Touroult-Jupin, P., Cremniter, J., Plouzeau, C., Faure, J.P., *et al.* (2020) First detection in *Helicobacter suis* of a mutation conferring resistance to

clarithromycin in *Helicobacter pylori*: case report and review of the literature. *Microb Drug Resist* **26:** 677–680.

Qiao, Y., Yan, J., Jia, J., Xue, J., Qu, X., Hu, Y., *et al.* (2019) Characterization of the biosynthetic gene cluster for the antibiotic armeniaspirols in *Streptomyces armeniacus*. *J Nat Prod* **82:** 318–323.

Savoldi, A., Carrara, E., Graham, D.Y., Conti, M., and Tacconelli, E. (2018) Prevalence of antibiotic resistance in *Helicobacter pylori*: a systematic review and meta-analysis in world health organization regions. *Gastroenterology* **155:** 1372–1382 e1317.

Scott, D.R., Marcus, E.A., Weeks, D.L., and Sachs, G. (2002) Mechanisms of acid resistance due to the urease system of *Helicobacter pylori*. *Gastroenterology* **123:** 187–195.

Sugano, K., Tack, J., Kuipers, E.J., Graham, D.Y., El-Omar, E.M., Miura, S., *et al.* (2015) Kyoto global consensus report on *Helicobacter pylori* gastritis. *Gut* **64:** 1353–1367.

Tanaka, M., Isogai, E., Isogai, H., Hayashi, S., Hirose, K., Kimura, K., *et al.* (2002) Synergic effect of quinolone antibacterial agents and proton pump inhibitors on *Helicobacter pylori*. *J Antimicrob Chemother* **49:** 1039–1040.

Thung, I., Aramin, H., Vavinskaya, V., Gupta, S., Park, J.Y., Crowe, S.E., and Valasek, M.A. (2016) Review article: the global emergence of *Helicobacter pylori* antibiotic resistance. *Aliment Pharmacol Ther* **43:** 514–533.

Trew, S.J., Wrigley, S.K., Pairet, L., Sohal, J., Shanu-Wilson, P., Hayes, M.A., *et al.* (2000) Novel streptopyrroles from *Streptomyces rimosus* with bacterial protein histidine kinase inhibitory and antimicrobial activities. *J Antibiot* **53:** 1–11.

Warren, J.R., and Marshall, B. (1983) Unidentified curved bacilli on gastric epithelium in active chronic gastritis. *Lancet* **1:** 1273–1275.

Xu, Y.F., Lian, D.W., Chen, Y.Q., Cai, Y.F., Zheng, Y.F., Fan, P.L., *et al.* (2017) In vitro and in vivo antibacterial activities of patchouli alcohol, a naturally occurring tricyclic sesquiterpene, against *Helicobacter pylori* infection. *Antimicrob Agents Chemother* **61:** e00122–e217.

Yonezawa, H., Osaki, T., and Kamiya, S. (2015) Biofilm formation by *Helicobacter pylori* and its involvement for antibiotic resistance. *Biomed Res Int* **2015:** 914791.

Yonezawa, H., Osaki, T., Fukutomi, T., Hanawa, T., Kurata, S., Zaman, C., *et al.* (2017) Diversification of the AlpB outer membrane protein of *Helicobacter pylori* affects biofilm formation and cellular adhesion. *J Bacteriol* **199:** e00729–e816.

Zanotti, G., and Cendron, L. (2019) Structural aspects of *Helicobacter pylori* antibiotic resistance. *Adv Exp Med Biol* **1149:** 227–241.

Zhang, R.G., Duan, G.C., Fan, Q.T., and Chen, S.Y. (2016) Role of *Helicobacter pylori* infection in pathogenesis of gastric carcinoma. *World J Gastrointest Pathophysiol* **7:** 97–107.

Supporting information

Additional supporting information may be found online in the Supporting Information section at the end of the article.
Fig. S1. Kill kinetics of *H. pylori* Hp159 by ARM1. Time- and dose-dependent killing of the bacteria by ARM1 (A) and MTZ (B) were evaluated. The MIC of ARM1 and MTZ was considered as 8 and 16 μg ml^{-1}, respectively. If no colonies

were present, calculations were made using the limit of detection (10^1 CFU ml^{-1}).

Fig S2. Development of resistance to ARM1 in *H. pylori* G27. The fold change was the normalized ratio of the MIC obtained for a given subculture to the MIC obtained for first-time exposure. ARM1 did not develop drug resistance over the 27 days of studies while metronidazole quickly acquired resistance on day 9. A representative of two independent experiments is shown.

Fig S3. Cell Cytotoxicity of ARM1 was assessed in human normal hepatocyte LO$_2$ cells. After overnight culture, cells were incubated with ARM1 at predetermined concentrations for 48 h and were then treated with CCK-8 reagent for assessment of cytotoxicity.

Fig S4. ARM1 had low toxicity *in vivo*. (A) After the mice were orally administrated with overdose (285 mg/kg, 10-fold effective dosage) ARM1 once a day for 5 consecutive days, the mice body weights were monitored daily for 7 days. (B) At the seven days after the last treatment, the mice were sacrificed, and the stomach, the liver, the spleen and the kidney were removed from the abdominal cavity and examined by H&E stain.

Table S1. The predicted Drug-like properties of ARM1.

Table S2. *In vitro* combinatory anti-*H. pylori* effect of ARM1 with each antibiotic.